### Title
A POUR IAYER, TWO INCH BORE, SUPERCONDUCTING DIPOLE MAGNET




### Author
Hassenzahl, W.V.



### Publication Date
1982-11-01

LBL-15372

Lawrence Berkeley Laboratory
UNIVERSITY OF CALIFORNIA

# Accelerator & Fusion Research Division

Presented at the 1982 Applied Superconductivity Conference, Knoxville, TN, November 28-December 3, 1982; and to be published in the Proceedings

A FOUR LAYER, TWO INCH BORE, SUPERCONDUCTING DIPOLE MAGNET

W.V. Hassenzahl, C. Peters, W. Gilbert, C. Taylor, and R. Meuser

November 1982

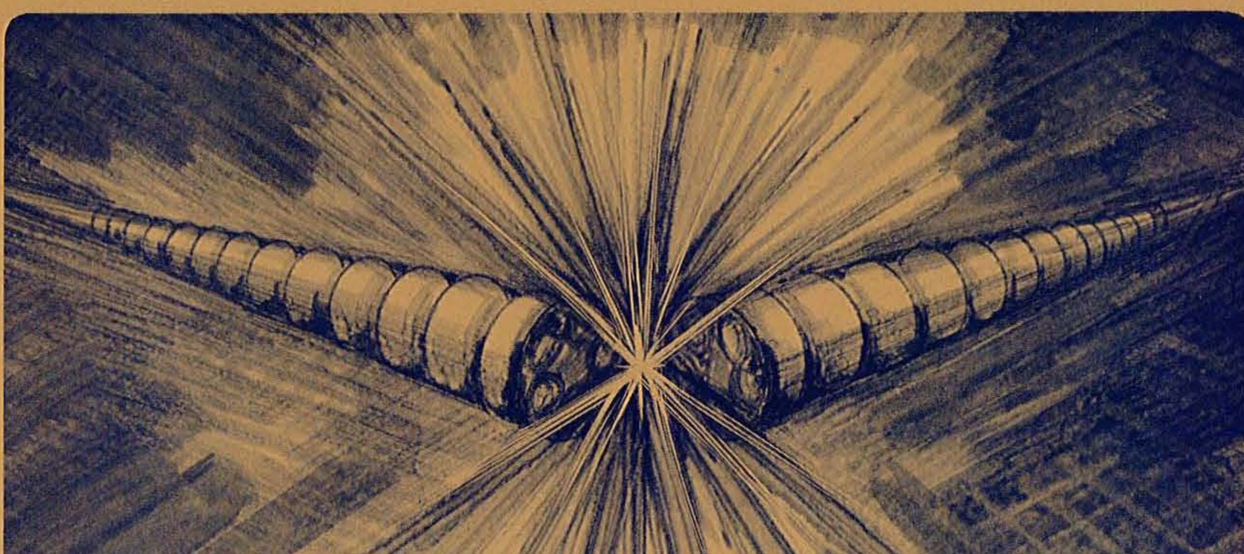

Prepared for the U.S. Department of Energy under Contract DE-AC03-76SF00098

LBL-14447
SUMAG-79

# A FOUR LAYER, TWO INCH BORE, SUPERCONDUCTING DIPOLE MAGNET*

W. V. Hassenzahl, C. Peters, W. Gilbert, C. Taylor, R. Meuser

November 1982

Accelerator and Fusion Research Division
Lawrence Berkeley Laboratory
University of California
Berkeley, California 94720

*This work was supported by the Director, Office of Energy Research, Office of High Energy and Nuclear Physics, High Energy Physics Division, U. S. Dept. of Energy, under Contract No. DE-AC03-76SF00098.

# A FOUR LAYER, TWO INCH BORE, SUPERCONDUCTING DIPOLE MAGNET*

W. V. Hassenzahl, C. Peters, W. Gilbert, C. Taylor and R. Meuser
Lawrence Berkeley Laboratory
University of California
Berkeley, CA 94720

## Introduction and Summary

Superconductors provide the accelerator designer with a unique opportunity to construct machines that can achieve high particle energies and yet have low operating costs. This paper describes the design, fabrication and testing of a 4 layer, 50 mm bore superconducting dipole magnet, D-9A. The magnet reached short sample, 5.8 T at 4.4 K and 8.0 T and 1.8 K, with little training, and exhibited low losses and low ramp rate sensitivity.

The optimum field for superconducting accelerator dipoles depends on many factors and cannot be determined in a general sense without the selection of a site and a variety of accelerator design parameters. The highest possible field must be considered if the circumference of any new accelerator is to be as small as possible to reduce the amount of land required for multi TeV accelerators, where new and interesting physics can be explored.

Two superconductors can be considered for a 10 T accelerator. The first is $Nb_3Sn$, which can operate at 10 T at about 4.4 K, and the second is NbTi, which must operate in superfluid helium at 1.8 K to achieve 10 T. Several different designs were considered for these magnets and two were selected as the basis for a model testing program.[1] The one described here, the cylindrical layer design, was selected because of the experience with this type of winding in the ESCAR,[2] the Fermilab[3] Doubler/Saver, the Brookhaven ISABELLE[4] magnets, and the recent results in the development and testing of model magnets at LBL.[5] A somewhat similar design was described by Ishibashi and McInturff.[6]

The 50 mm (2") bore was selected for these models to minimize costs. Accelerator design does not require larger bores, and we selected 50 mm (2") as a reasonable goal with existing conductors. Smaller bore magnets of the layer type would be quite difficult with the conductor used for D-9A because of the small radius of curvature of the inside turn of the first layer.

Our program to develop 10 Tesla coils includes perfecting the 4 layer design including fabrication and assembly and developing a suitable conductor. The general conductor type selected is a Rutherford cable of approximately the width of the FNAL cable. To achieve 10 T in 4 layers with NbTi at 1.8 K requires an efficient coil design with graded conductor and a copper to superconductor ratio of about 1. We are now developing suitable graded cable. However we used the cable with the lowest copper-to-superconductor ratio available, 1.5, in the model dipoles described here. The current density is the same in all four layers.

## Coil Design

The 4 layer magnet, D-9A, described here is a logical extension of work on 2 and 3 layer magnets already developed at LBL.[7-9] A transverse cross section of the coil is shown in Fig. 1, and a

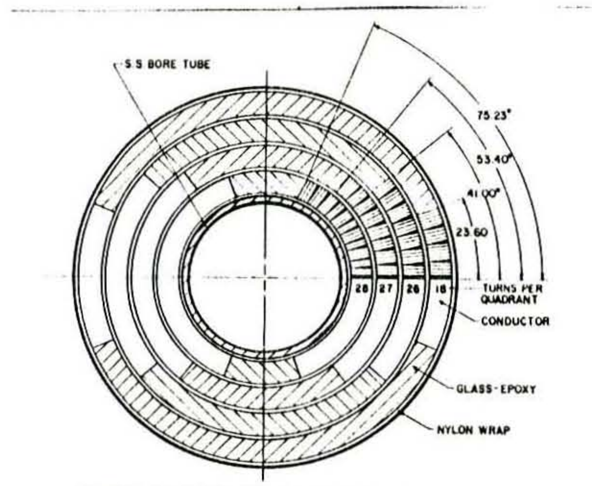


CROSS SECTION OF 4 LAYER DIPOLE D-9A
XBL 8211-1329

Fig. 1. Cross section of the D-9A Dipole.

longitudinal section is shown in Fig. 2. Some characteristics of the coil are presented in Table I. The central angles for the four layers are chosen to minimize the allowable harmonics with the wedges as shown. The actual conductor dimensions are slightly different fom those used in the optimization so some harmonics may appear but these could easily be eliminated in a large scale production with consistent conductor dimensions.

TABLE I: Accelerator dipole D-9A design characteristics

| Layer | Turns | ID (mm) | OD (mm) | Pole Angle (°) | Circumferential Modulus (MPa) |
|---|---|---|---|---|---|
| 1 | 28 | 58.5 | 74.5 | 75.23 | $1.83 \times 10^4$ |
| 2 | 27 | 76.7 | 92.8 | 53.40 | $2.03 \times 10^4$ |
| 3 | 26 | 94.9 | 110.9 | 41.00 | $2.17 \times 10^4$ |
| 4 | 18 | 113.0 | 129.0 | 23.60 | $2.39 \times 10^4$ |

The coil winding can support an inward radial load in the straight section and when clamped under the maximum stress remains separated from the stainless steel boretube by about 0.5 mm. A layer of 1 mm thick nylon monofilament is wound over each layer to (1) provide a precompression before the subsequent layers are applied, (2) aid the external rings in supplying the final preload, and to (3) provide a path for helium to flow circumferentially around the coil. The ends of the coil, which are not self supporting, contact the boretube and are under a radial load and some circumferential load due to the nylon banding and external rings.

*This work was supported by the Director, Office of Energy Research, Office of High Energy and Nuclear Physics, High Energy Physics Division, U. S. Dept. of Energy, under Contract No. DE-AC03-76SF00098.

Manuscript received November 30, 1982

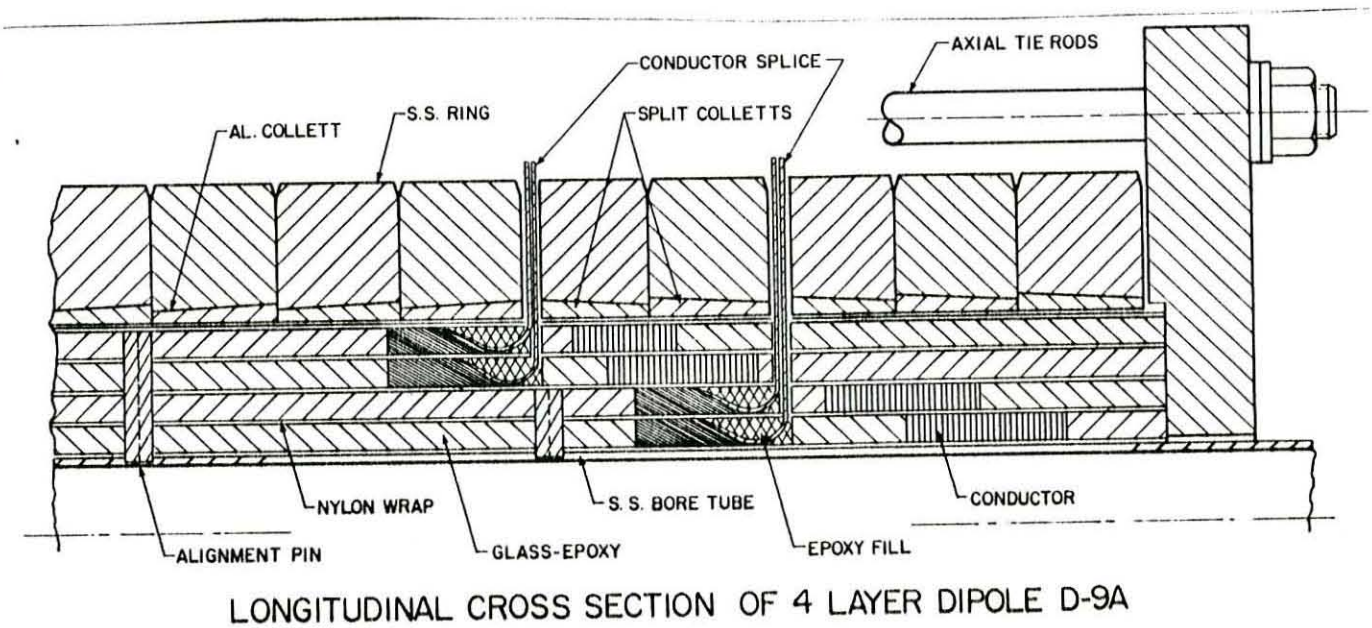


Fig. 2. Longitudinal cross section of the D-9A winding showing the end of coil and the staggered layer ends, which reduce the field rise.

TABLE II: Stresses in the 4 layers of the D-9A dipole under various conditions

| Layer | During Cure (MPa) | After Final Assy (MPa) | At 1.8 K (MPa) | At Max Current (MPa) |
|---|---|---|---|---|
| 1 | 82.7 | 89.6 | 68.9 | 98.6 |
| 2 | 82.7 | 65.5 | 51.7 | 73.8 |
| 3 | 82.7 | 51.7 | 44.8 | 60.7 |
| 4 | 82.7 | 33.1 | 33.1 | 37.2 |

The longitudinal section in Fig. 2 shows that the ends of the coil layers are staggered, the outer coils are shorter, to reduce the maximum field at the innermost turn of the first layer. The effect of this end design is to move the high field region to the straight section of layer one, probably below the ends of the straight section of the innermost turns of layers three and four. Neglecting these possible end effects, the maximum field rise in the straight section of layer 1 is about 3 on the first turn.

The 2.46 mm thick, 52.5 mm diam bore tube is an integral part of the coil and is vacuum tight. Pins, as shown in Fig. 2 are welded into holes in this tube to provide an index for mounting the preassembled coils halves and to support the coil against the circumferential force of the nylon during winding. The field quality of this magnet was not measured during the first test, but the integral, sealed bore tube will allow cold measurement at a later time if necessary.

The conductor used in the coils is similar to the FNAL Rutherford cable and is described in Table III. The copper-to-superconductor ratio in the conductor is 1.5, which is somewhat lower than that of the FNAL Doubler/Saver conductor. The short-sample critical currents of this conductor are shown in Fig. 3 at both 4.4 and 1.8 K.[10] Several different measurements were combined to obtain these curves, some were on single strands, others on complete cable. The results are all generally in agreement, and the values for 4.4 K are probably correct to about 5 .

TABLE III: Conductor used for accelerator dipole D9A

| | |
|---|---|
| Conductor dimensions $(mm)^2$ insulated at 82.7 MPa | 1.25 x 8.03 |
| Kapton insulation $(mm)^2$ 50 overlap | 0.025 x 12.7 |
| No. strands | 23 |
| Cable pitch $(mm^{-1})$ | 0.013 |
| Strand diam. (mm) | 0.027" |
| Twist pitch $(mm^{-1})$ | 0.11 |
| Copper to superconductor ratio | 1.5 |

The 1.8 K curve is based on a few points between 10 and 11.5 T and is an extrapolation to the actual operating conditions near 8.0 T. The load lines for the central and estimated peak fields in the coil are also shown.

The cable is very lightly compacted by a "turk's head" while in the winding line under tension. This operation produces a rectangular conductor with a final size that is uniform throughout the coil and brings the internal structure of the conductor into final registry to remove distortions that might have been introduced during handling. For example, in the year or so between manufacture and coil winding the conductor may be respooled several times and passed over several pulleys during the cleaning and inspection process. This final compaction and sizing is quite important because of the strong dependence of the coil prestress on the conductor dimensions. Glass-epoxy wedges are placed in the windings of each layer at intervals of about 7.5° of winding arc. This keeps the conductors oriented radially and maintains constant circumferential pressure across each layer. The winding package has a measured effective circumferential modulus of about $2\times10^4$ MPa as shown in Table I. This relatively high value, compared to the stress in earlier

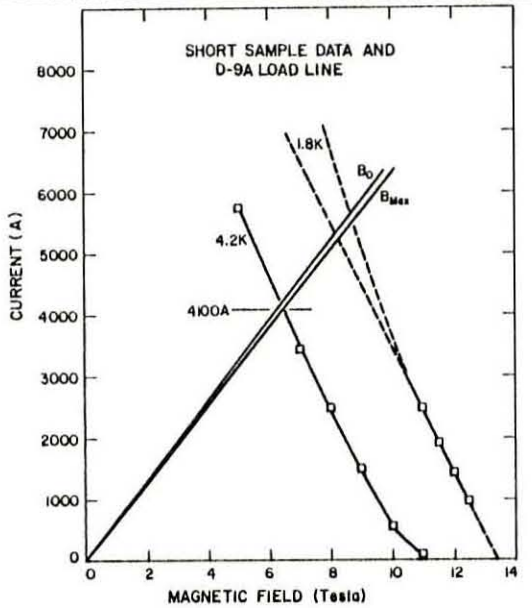


Fig. 3. Short sample critical current for the conductor used in D-9A and the D-9A load line.

coils,[5,7] imposes severe restrictions on the dimensional tolerance of the conductor. Using the first layer as an example, assuming the circumference is held constant, a variation of 2.54 μm (0.0001") in the conductor thickness leads to a 28 Mpa (4000 psi) change in the compressive load.

After compaction, the conductor passes through a wrapping stage where a spiral wrap of Kapton insulation is applied. The Kapton layer is overlapped to give a 50 μm (0.002") insulation thickness over about 90 of the conductor surface. As a final step, B-stage epoxy is then sprayed onto one surface of the insulated conductor before it is wound onto the coil form. The epoxy applied in this fashion aids in fabrication but has little effect on the coil under load, and no epoxy is in direct contact with the conductor.

During coil winding the conductor is under about 450 N (100 lbs.) tension. A dummy pole island made of aluminum is used for the winding and the epoxy curing processes. This island is firmly attached to a solid cylindrical mandrel. Wedges of glass-epoxy are placed between the turns as the conductor is wound onto the mandrel and the island. After winding is completed an aluminum half-shell having the same ID and OD as the layer is mated to the winding and mandrel. A stainless steel shell and chain clamps are then applied to the entire assembly. The coil winding is compressed, but the dimensions of the backing aluminum half shell are chosen to keep the coil away from the mandrel. The pressure in the coil is brought up to 83 Mpa (12,000 psi) and the entire assembly is placed in an oven and cured at 120°C for about 3 hours. The bolts holding the chains in place are periodically tightened to maintain pressure as the epoxy cures and the Kapton insulation creeps into the spaces around the conductor. The creep is usually completed in the first hour of curing.

The assembly of the four coil layers is a sequential operation in which each layer is mounted in place and the nylon is then wrapped on at the design pressure given in Table I. Figure 4 shows the first layer during assembly.

Target prestresses were determined for each layer. The goal was to provide sufficient ambient temperature precompression so that after cooldown and upon energizing, the inside turns of each layer would remain under compression. Precompression has to be high enough to offset stress loss due to thermal contraction and to the Lorentz forces tending to move conductor away from the poles. The magnet was modeled as a series of nesting shells of different mechanical and thermal characteristics that depend on the amount of G-10 and superconductor in each layer to calculate the stress change during cooldown. A different calculation determined the uniform circumferential compression that produces, at the first turn, the same motion as the Lorentz force. These

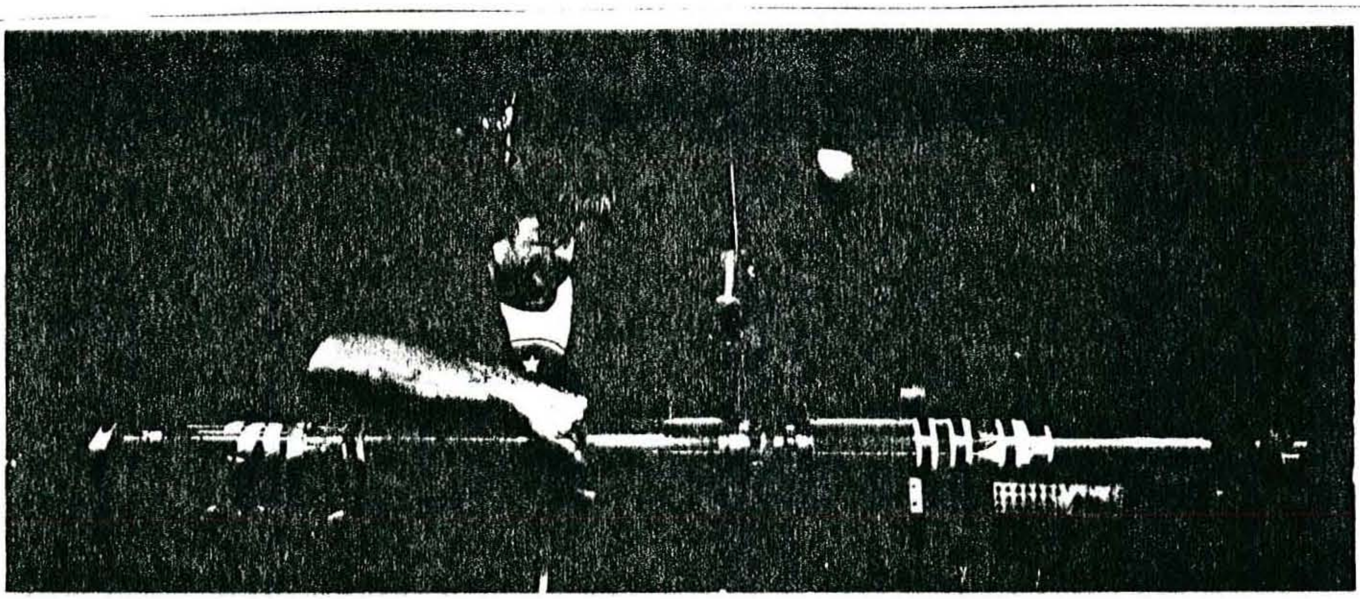

Fig. 4. The first layer of D-9A during coil assembly.

two stresses are superimposed (added) to give the minimum assembly prestress for each layer.

For example, in layer 1, cooldown to 4 K will cause the compessive stress to decrease by 3,000 psi. The Lorentz force, assuming a zero initial compression, would cause the first turn to move tangentially 0.071 mm away from the pole. Had this layer been compressed initially by this amount, corresponding to 56.5 Mpa (8200 psi), there would have been no motion of the first turn. The two effects combine to give a minimum target prestress of 11,200 psi. We used 13,000 psi as our goal for this layer.

During assembly, after each new pair of preformed layer halves is assembled onto the existing layers, a radial pressure is applied via chain clamps to produce a compressive stress in each layer. The mid-plane spacers in the new layer are adjusted to tailor its compressive prestress to the target value relative to the inner layers. This distribution of stresses is maintained as subsequent layers are assembled and when the external structural rings are applied. The nylon monofilament wrap between each layer does not alter this distribution. Stresses are measured using strain gage instrumented aluminum blocks fit into slots in the pole island of each layer. Each block, which is about 3 x 6 x 25 $mm^3$, is instrumented with a full-bridge strain-gage circuit.

The compressive loads expected in the coil as constructed are shown in Fig. 5. These loads are large enough to prevent separation of the conductor from the pole islands when the coil is fully charged. The pressures in the coil under other various conditions are also shown in Fig. 5.

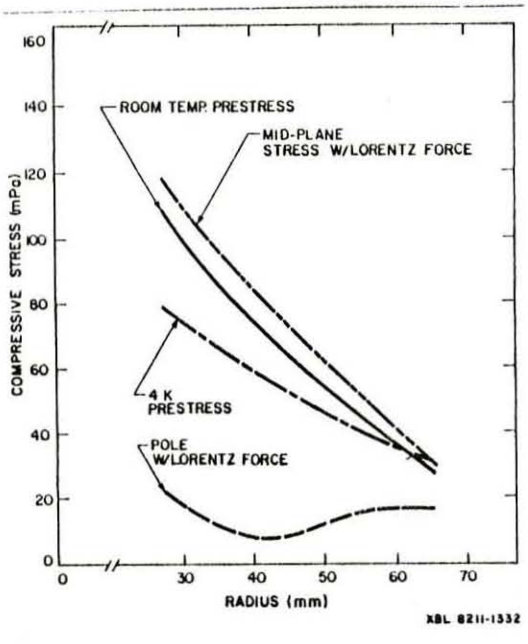


Fig. 5 Compressive loads in the D-9A coil under various conditions.

Finally, after the four conductor layers and the four nylon wraps are completed, a set of stainless steel rings and collets are assembled on the outside of the coil to bring the pressures in the winding to the design value. The rings also resist the Lorentz forces in the coil during operation.

The splices between layers 1 and 2 and layers 3 and 4 are made outside the coil as shown in Figs. 2 and 4. To allow the conductor to cross to the outside of the rings and to avoid damaging the conductor during assembly, the rings are installed in both directions from the point where the layer 3 and layer 4 leads leave the coil. The two collets between the two lead areas are split to pass over the conductors without damaging the insulation. The completed coil is shown in Fig. 6.

## Test Results

The D-9A dipole magnet was tested in our horizontal He I/He II test cryostat that has been described previously.[5,7] The training behavior in both He I and pressurized He II is excellent; short sample performance in He I at 4.4 K was reached on the third quench. The sequence was 4.8 T central field on the first quench, 5.3 T on the second and 5.8 T on the third. In pressurized He II at 1.8 K short sample was reached on the second quench. The sequence was 7.4 T on the first quench and 8.0 T on the second.

Voltage taps on the inner turns of the inside layer showed that the quenches all started in the

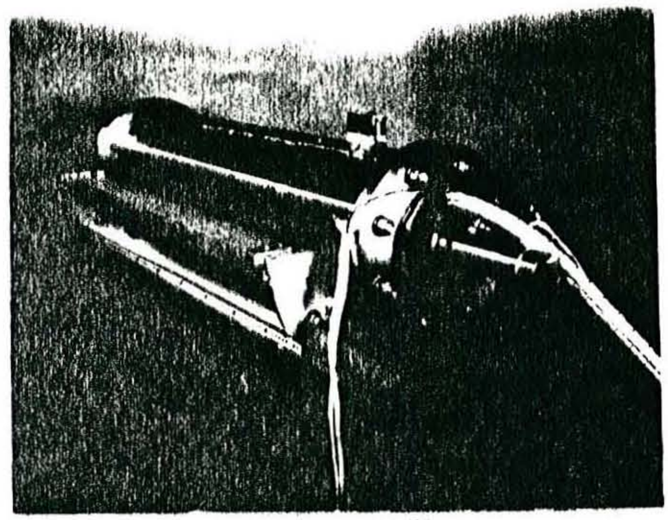

Fig. 6. The completed D-9A coil

straight section of the inside turn of either the top or bottom half of the inner layer. although a relatively lossy cable utilizing "staybrite" insulation on the strands is used, the ramp rate sensitivity is relatively low at both 4.4 and 1.8 K. We attribute this to adequate helium ventilation.

Extensive cyclic heating data were taken. In He II, we use a calorimetric method using the rise in bath temperature as an indication of energy loss.[11] Cycling was done in the range from 0 to 6.1 T with field change rates beween 0 and 1 T per second. At the maximum rate the cyclic loss was 37.4 W. In He I a computer based electronic system was used. The magnet was cycled from 0.3 to 4.6 T at rates ranging from 0 to 0.9 T per second at the maximum rate in He II, the cyclic loss was 30.4 W.

Acknowledgements

The authors wish to acknowledge the efforts of J. O'Neill, R. Hannaford, A. Borden, R. Althaus, J. Rechen, and S. Caspi in the fabrication and testing of the D-9A magnet.

References

1. C. Taylor, R. Meuser, S. Caspi, W. Gilbert, W. Hassenzahl, C. Peters, R. Wolgast, "High-Field Superconducting Accelerator Magnets," Lawrence Berkeley Laboratory Report LBL-14400. Also presented at the ICEC, Kobe, May 1982.

2. G. R. Lambertson, W. S. Gilbert, J. B. Rechen, "Final Report on the Experimental Superconducting Synchrotron (ESCAR)," published in Particle Accelerators, Vol. 10, Numbers 3-4 (1980), also LBL-8211.

3. "A Report on the Design of the Fermi National Accelerator Laboratory Superconducting Accelerator" Fermilab Report - May 1979.

4. R. B. Palmer et al., "The Two Layer ISABELLE Cable Magnet," BNL Internal Report TLM α23, Sept. 1981.

5. C. Taylor, R. Althaus, S. Caspi, W. S. Gilbert, W. Hassenzahl, R. Meuser, J. Rechen and R. Warren, "A Novel Epoxy-Free Construction Method for Fabricating Dipole Magnets and Test Results," IEEE Trans. on Nuclear Science, Vol. NS-28, No. 3, Part 2, June 1981, also LBL-11752.

6. K. Ishibashi and A. D. McInturff, "Stress Analysis of Superconducting 10-T Magnets for Synchrotrons," presented at the ICEC, Kobe, May 1982.

7. C. Taylor et al., "Design of Epoxy-Free Superconducting Dipole Magnets and Performance in Both Helium I and Pressurized Helium II," IEEE Trans. on Magnetics, Vol. MAG-17, No. 5, Sept. 1981, also LBL-12455.

8. W. Hassenzahl et al., "Stability in Accelerator Dipoles in He I and He II," Proceedings of the workshop held at Saclay (France), Nov. 16-19, 1981, International Institute of Refrigeration, Commission A 1/2.

9. C. Taylor et al., "Alternative Dipole Magnets for ISABELLE," 9th International Cryogenic Engineering Conference, Kobe, Japan, May 11-14, 1982.

10. Short sample measurements of the 213 strand "Rutherford" cable were made by Dr. Yukikazu Iwasa of M.I.T.'s Francis Bitter National Magnet Laboratory in the field range from 8 to 12.5 tesla, and in the temperature range from 1.8 to 4.2 K. Other measurements at 4.2 K were made at LBL.

11. S. Caspi, "The Use of Calorimetry in Superfluid He-II to Measure Losses in Superconducting Magnets," 9th Inter, Cryo. Engr. Conf., Kobe, Japan, 1982.